PN 005

)PAL INTERNAL PHYSICS NOTE 90-05

NEUTRAL HEAVY LEPTON ANALYSIS

This is a new analysis, to be presented at the Washington APS meeting and soon to become a CERN preprint. The Heavy Lepton Group is releasing it now as a Physics Note for comments and approval for presentation. It is expected that the CERN preprint will be ready in about ten days.

The Editorial Board has approved this note for release to the OPAL collaboration, but with two caveats: First, in the ν–L^0 analysis, presented in Figures 4-b, 5-b, and 6, the Editorial Board (and the Heavy Lepton Working Group) believes that the uncertainties in filter and trigger efficiency for masses m_{L^0} greater than 75 GeV/c^2 need some additional work – the errors in the acceptance in this region may be underestimated. Increasing the errors on the acceptance will have a small effect and will only affect the very high-mass region. We expect that any change in the contours will be less than 10%. The Editorial Board believes that the region above 75 GeV/c^2 should not be presented at the APS meeting unless additional work is done.

Second, the TIPTOP event generator treats radiation to first order only with no exponentiation of soft photons. Because of this deficiency, the calculated cross section was reduced by 30% in determining the mass limits for the production of heavy neutral lepton pairs. More work must be devoted to checking this calculation before we will feel fully confident in these limits.

The paper is being released to the collaboration now for comments. Please send comments to KROLL@CERNVM by Friday, April 13, at 5:00pm.

EUROPEAN ORGANIZATION FOR NUCLEAR RESEARCH

CERN–EP/90–xxx
14 March,1990

Limits on Neutral Heavy Lepton Production from Z^0 Decay

The OPAL Collaboration

M.Z. Akrawy[11], G. Alexander[21], J. Allison[14], P.P. Allport[5], K.J. Anderson[8], J.C. Armitage[6],
G.T.J. Arnison[18], P. Ashton[14], G. Azuelos[16], J.T.M. Baines[14], A.H. Ball[15], J. Banks[14],
G.J. Barker[11], R.J. Barlow[14], J.R. Batley[5], G. Bavaria[16], F. Beck[7], K.W. Bell[18], G. Bella[21],
S. Bethke[10], O. Biebel[3], I.J. Bloodworth[1], P. Bock[10], H. Breuker[7], R.M. Brown[18], R. Brun[7],
A. Buijs[7], H.J. Burckhart[7], P. Capiluppi[2], R.K. Carnegie[6], A.A. Carter[11], J.R. Carter[5],
C.Y. Chang[15], D.G. Charlton[7], J.T.M. Chrin[14], I. Cohen[21], J.E. Conboy[13], M. Couch[1],
M. Coupland[12], M. Cuffiani[2], S. Dado[20], G.M. Dallavalle[13], O.W. Davies[14], M.M. Deninno[2],
A. Dieckmann[10], M. Dittmar[4], M.S. Dixit[17], D. Duchesneau[16], E. Duchovni[24], I.P. Duerdoth[7,c],
D. Dumas[6], H. El Mamouni[16], P.A. Elcombe[5], P.G. Estabrooks[6], E. Etzion[21], F. Fabbri[2],
P. Farthouat[19], H.M. Fischer[3], D.G. Fong[15], M.T. French[18], C. Fukunaga[22], B. Gandois[19],
O. Ganel[24], J.W. Gary[10], N.I. Geddes[18], C.N.P. Gee[18], C. Geich-Gimbel[3], S.W. Gensler[8],
F.X. Gentit[19], G. Giacomelli[2], W.R. Gibson[11], J.D. Gillies[18], J. Goldberg[20], M.J. Goodrick[5],
W. Gorn[4], D. Granite[20], E. Gross[24], P. Grosse-Wiesmann[7], J. Grunhaus[21], H. Hagedorn[9],
J. Hagemann[7], M. Hansroul[7], C.K. Hargrove[17], J. Hart[5], P.M. Hattersley[1], D. Hatzifotiadou[7],
M. Hauschild[7], C.M. Hawkes[7], E. Heflin[4], J. Heintze[10], R.J. Hemingway[6], R.D. Heuer[7], J.C. Hill[5],
S.J. Hillier[1], P.S. Hinde[14], C. Ho[4], J.D. Hobbs[8], P.R. Hobson[23], D. Hochman[24], B. Holl[7],
R.J. Homer[1], S.R. Hou[15], C.P. Howarth[13], R.E. Hughes-Jones[14], P. Igo-Kemenes[10], M. Imori[22],
D.C. Imrie[23], A. Jawahery[15], P.W. Jeffreys[18], H. Jeremie[16], M. Jimack[7], E. Jin[4,b], M. Jobes[1],
R.W.L. Jones[11], P. Jovanovic[1], D. Karlen[6], K. Kawagoe[22], T. Kawamoto[22], R.G. Kellogg[15],
B.W. Kennedy[13], C. Kleinwort[7], D.E. Klem[17], G. Knop[3], T. Kobayashi[22], L. Köpke[7], T.P. Kokott[3],
M. Koshiba[22], R. Kowalewski[6], H. Kreutzmann[3], J. von Krogh[10], J. Kroll[8], P. Kyberd[11],
G.D. Lafferty[14], F. Lamarche[16], W.J. Larson[4], M.M.B. Lasota[11], J.G. Layter[4], P. Le Du[19],
P. Leblanc[16], D. Lellouch[7], P. Lennert[10], L. Lessard[16], L. Levinson[24], S.L. Lloyd[11],
F.K. Loebinger[14], J.M. Lorah[15], B. Lorazo[16], M.J. Losty[17], J. Ludwig[9], J. Ma[4,b], A.A. Macbeth[14],
M. Mannelli[7], S. Marcellini[2], G. Maringer[3], J.P. Martin[16], T. Mashimo[22], P. Mättig[7], U. Maur[3],
T.J. McMahon[1], A.C. McPherson[6], F. Meijers[7], D. Menszner[10], F.S. Merritt[8], H. Mes[17],
A. Michelini[7], R.P. Middleton[18], G. Mikenberg[24], D.J. Miller[13], C. Milstene[21], M. Minowa[22],
W. Mohr[9], A. Montanari[2], T. Mori[22], M.W. Moss[14], A. Muller[19], P.G. Murphy[14], W.J. Murray[5],
B. Nellen[3], H.H. Nguyen[8], M. Nozaki[22], A.J.P. O'Dowd[14], S.W. O'Neale[7,d], B. O'Neill[4],
F.G. Oakham[17], F. Odorici[2], M. Ogg[6], H. Oh[4], M.J. Oreglia[8], S. Orito[22], G.N. Patrick[18],
S.J. Pawley[14], J.E. Pilcher[8], J.L. Pinfold[24], D.E. Plane[7], B. Poli[2], A. Possoz[8,e], A. Pouladdej[6],
T.W. Pritchard[11], G. Quast[7], J. Raab[7], M.W. Redmond[8], D.L. Rees[1], M. Regimbald[16], K. Riles[4],
C.M. Roach[5], F. Roehner[9], A. Rollnik[3], J.M. Roney[8], A.M. Rossi[2,a], P. Routenburg[6], K. Runge[9],
O. Runolfsson[7], S. Sanghera[6], R.A. Sansum[18], M. Sasaki[22], B.J. Saunders[18], A.D. Schaile[9],

O. Schaile[9], W. Schappert[6], P. Scharff-Hansen[7], H. von der Schmitt[10], S. Schreiber[3], J. Schwarz[9], A. Shapira[24], B.C. Shen[4], P. Sherwood[13], A. Simon[3], G.P. Siroli[2], A. Skuja[15], A.M. Smith[7], T.J. Smith[1], G.A. Snow[15], E.J. Spreadbury[13], R.W. Springer[15], M. Sproston[18], K. Stephens[14], J. Steuerer[9], H.E. Stier[9], R. Ströhmer[10], D. Strom[8], H. Takeda[22], T. Takeshita[22], T. Tsukamoto[22], M.F. Turner[5], G. Tysarczyk[10], D. Van den plas[16], G.J. VanDalen[4], C.J. Virtue[17], A. Wagner[10], C. Wahl[9], H. Wang[4,b], C.P. Ward[5], D.R. Ward[5], J. Waterhouse[6], P.M. Watkins[1], A.T. Watson[1], N.K. Watson[1], M. Weber[10], S. Weisz[7], N. Wermes[7], M. Weymann[9], G.W. Wilson[7], J.A. Wilson[1], I. Wingerter[7], V-H. Winterer[9], N.C. Wood[13], S. Wotton[7], B. Wuensch[3], T.R. Wyatt[14], R. Yaari[24], H. Yamashita[22], Y. Yang[4,b], G. Yekutieli[24], W. Zeuner[7], G.T. Zorn[15], S. Zylberajch[19].

[1]School of Physics and Space Research, University of Birmingham, Birmingham, B15 2TT, UK
[2]Dipartimento di Fisica dell' Universita di Bologna and INFN, Bologna, 40126, Italy
[3]Universität Bonn, D-5300 Bonn 1, FRG
[4]Department of Physics, University of California, Riverside, CA 92521 USA
[5]Cavendish Laboratory, Cambridge, CB3 0HE, UK
[6]Carleton University, Dept of Physics, Colonel By Drive, Ottawa, Ontario K1S 5B6, Canada
[7]CERN, European Organisation for Particle Physics, 1211 Geneva 23, Switzerland
[8]Enrico Fermi Institute and Dept of Physics, University of Chicago, Chicago Illinois 60637, USA
[9]Fakultät für Physik, Albert Ludwigs Universität, D-7800 Freiburg, FRG
[10]Physikalisches Institut, Universität Heidelberg, D-6900 Heidelberg, FRG
[11]Queen Mary and Westfield College, University of London, London, E1 4NS, UK
[12]Birkbeck College, London, WC1E 7HV, UK
[13]University College London, London, WC1E 6BT, UK
[14]Department of Physics, Schuster Laboratory, The University, Manchester M13 9PL, UK
[15]Dept. of Physics and Astronomy,University of Maryland, College Park, Maryland 20742, USA
[16]Laboratoire de Physique Nucleaire, Universite de Montreal, Montreal, Quebec, H3C 3J7, Canada
[17]National Research Council, Herzberg Institute of Astrophysics, Ottawa, Ont. K1A 0R6, Canada
[18]Rutherford Appleton Laboratory, Chilton, Didcot, Oxfordshire, OX11 0QX, UK
[19]DPhPE, CEN Saclay, F-91191 Gif-sur-Yvette France
[20]Department of Physics, Technion-Israel Institute of Technology, Haifa 32000, Israel
[21]Department of Physics and Astronomy, Tel Aviv University, Tel Aviv 69978, Israel
[22]Int. Center for Elementary Particle Phys. and Dept. of Phys., Univ. of Tokyo and Kobe University, Tokyo 113, Japan
[23]Brunel University, Uxbridge, Middlesex, UB8 3PH ,UK
[24]Nuclear Physics Department, Weizmann Institute of Science, Rehovot, 76100, Israel

[a]Present address: Dipartimento di Fisica, Universita della Calabria, 87036 Rende, Italy
[b]On leave from Harbin Institute of Technology, Harbin, China
[c]On leave from Manchester University
[d]On leave from Birmingham University
[e]Present address: EPFL, Lausanne

(Submitted to Physics Letters)

Abstract

Data taken with the OPAL detector at LEP during a scan of the Z^0 resonance were searched for evidence of production of neutral heavy leptons that decay via mixing. Four different mixing modes of the neutral heavy lepton are considered: $L^0 \rightarrow e\ W^*$,$L^0 \rightarrow \mu\ W^*$, $L^0 \rightarrow \tau\ W^*$, and $L^0 \rightarrow \nu\ Z^*$. No evidence is seen of a neutral heavy lepton signal; branching fraction limits are set for $Z^0 \rightarrow L^0 \overline{L^0}$ and for $Z^0 \rightarrow \nu\ \overline{L^0}$ (or $\overline{\nu} L^0$) relative to $Z^0 \rightarrow$hadrons. Depending on the assumed neutral-heavy-lepton decay mode and mass, limits on this ratio in the range of 10^{-3} to 10^{-4} are obtained.

1 Introduction

A feature of many extensions to the standard model is the existence of neutral heavy leptons. Many experimental searches have been made for such objects [1]. This paper presents results of a search for neutral heavy lepton in the data of the OPAL detector [2] taken in scans at the Z^0 peak. The acceptance corrected number of hadronic events in the data sample used in this search is 24275.

Our purpose is to make a general search for neutral heavy lepton events in Z^0 decays. The event signatures we search for are motivated by three models of neutral heavy lepton production and decay (following a review by Gilman [3]).

- Fourth Generation With Mixing
  The model contains a fourth generation of quarks and leptons, including right-handed singlet fields for the neutrinos. The weak eigenstates are mixtures of the mass eigenstates (ν_j). For example,
  $$\nu_e = \sum_{j=1}^{4} U_{ej}\nu_j,$$
  and the neutral heavy lepton will decay via mixing in the charged-current mode ($L^0 = \nu_4$):
  $$L^0 \rightarrow l\ W^* \quad l\ =\ e\ \mu \text{ and/or } \tau$$
  (the fourth generation charged lepton is assumed to be heavier than the fourth generation neutrino). Neutral-current decays $L^0 \rightarrow \nu_l Z^*$ are forbidden by the GIM mechanism. For M_4 less than half the Z^0 mass, the neutral heavy lepton is produced via
  $$e^+e^- \rightarrow L^0\overline{L^0} \qquad (1)$$
  with the same cross section as light neutrinos (except for phase space factors).

- See–Saw Model
  Each left-handed neutrino has a massive right-handed singlet partner. The light neutrinos mix with the heavy neutral singlets. The neutral heavy leptons do not couple directly to the Z^0 but for $M_L < M_z$ one expects production through
  $$e^+e^- \rightarrow \nu\ \overline{L^0} \text{ or } \bar{\nu}L^0 \qquad (2)$$
  where the cross section is reduced from the cross section for light-neutrino pair-production by a phase–space factor and the square of the mixing amplitude (the cross section for pair-production of heavy neutrinos is reduced by the fourth power of the mixing amplitude). The neutral heavy lepton can decay through both charged-current and neutral-current modes since no GIM suppression operates between the left-handed and right-handed sectors.
  $$L^0 \rightarrow l\ W^* \qquad (3)$$
  $$L^0 \rightarrow \nu_l Z^* \qquad (4)$$
  $$l\ =\ e\ \mu \text{ and/or } \tau$$

- Mirror Lepton Model
  The mirror sector consists of right-handed doublets and left-handed singlets. For $M_L < M_z/2$ one expects production through reaction (1). Depending on the model, subsequent decays may occur in the mirror sector or through mixing into the standard sector. Both charged-current (3) and neutral-current (4) decays are allowed.

More detailed discussions of models containing neutral heavy leptons can be found in [3] [4] [5]. In this report we present results of a search for events from reaction (1) and (2) and for both charged-current and neutral-current decays of the neutral heavy lepton.

Before discussing the search for direct evidence of heavy neutral leptons, it is interesting to consider the implications of the OPAL Z^0 line shape measurement [6]. The current OPAL line shape measurement yields an invisible width of Γ_{inv}=453±44 MeV and a total width of Γ_Z=2536±45 MeV. Figure 1 shows the partial width $\Gamma(Z^0 \rightarrow L^0 \overline{L^0})$ for production of neutral heavy leptons through reaction (1) with standard model coupling. A 2 σ upper limit on Γ_{inv} is 541 MeV. The invisible width of three light neutrinos plus a stable neutral heavy lepton would be greater than 541 MeV if the heavy lepton had a mass less than 42.3 GeV/c^2. Whether or not it is stable, a neutral heavy lepton would also increase the total width. A 2 σ upper limit on the total width measurement excludes a neutral heavy lepton for M_L<22 GeV/c^2. A direct search can set a much more stringent limit for unstable neutral heavy leptons. A 1 MeV increase in the Z^0 width corresponds to the production of 14 events in this data sample.

2 The Detector

The data were recorded with the OPAL detector at the CERN e^+e^- collider, LEP, during the Fall 1989 run. Detailed descriptions of the OPAL detector have been presented elsewhere [2] [9]. The detector consists of 6 main subsystems. These are

1. A central drift chamber system inside a 6.16m by 4.0m diameter solenoidal magnet which produces a 0.43 Tesla field. The central drift chamber system consists of a high–precision vertex chamber, a main jet chamber with 159 axial sense wires (r-ϕ measurement) with dE/dx and current division (z–coordinate) readout, and z–chambers (z-coordinate).

2. A time–of–flight system (TOF) consisting of 160 scintillation counters. These counters cover the surface of the magnet coil.

3. An electromagnetic calorimeter, surrounding the magnet, composed of a presampler and lead–glass counter array. The lead–glass array consists of 9440 blocks (10 x 10 cm) in the barrel region and 1123 blocks in each of the two endcaps.

4. A hadron calorimeter composed of limited streamer and proportional chambers embedded in the barrel and endcap flux return iron of the magnet.

5. A muon chamber system comprised of four layers of large drift chambers surrounding the detector.

6. A system of luminosity monitors composed of lead–scintillator calorimeters and proportional tubes. These forward detectors cover angles around the beams from 39 to 155 mrad.

The triggers used in this analysis are based on four independent detector components: the electromagnetic calorimeter, the time–of–flight system, the jet chamber, and the barrel muon chambers. The calorimeter trigger requires an energy sum of at least 6 GeV in the lead–glass barrel or in one endcap, and the TOF trigger requires hits in at least three nonadjacent time–of–flight counters. A track trigger for charged particles requires that at least two jet–chamber tracks must originate from the vertex in the r-z projection, each with a minimum transverse momentum of 450 MeV/c. In addition, an event is recorded if a track found in the barrel muon chambers (with three out of four planes) is associated within 260 mrad in azimuth with either a signal in a TOF scintillator or a track found in the central detector. The calorimeter, TOF, and track triggers are independent, which allows a cross–check of trigger efficiencies.

All events were passed through an on-line event filter [9] to reject trivial backgrounds. The efficiency for neutral heavy lepton events to pass both the trigger and filter selection has been determined from Monte Carlo studies and is included in the overall selection efficiency.

3 Analysis

Two methods are used to search for neutral heavy leptons:

1. a search for events with large missing energy and transverse momentum
2. a search for events with an isolated lepton (e or μ) together with a second isolated track

Eight combinations of production and decay modes of neutral heavy leptons have been studied. These combinations and the corresponding search methods are

- $e^+e^- \rightarrow L^0\overline{L^0}$
    - $L^0 \rightarrow e\ W^*$ isolated track search
    - $L^0 \rightarrow \mu\ W^*$ isolated track search
    - $L^0 \rightarrow \tau\ W^*$ isolated track search
    - $L^0 \rightarrow \nu\ Z^*$ missing energy and p_t
- $e^+e^- \rightarrow \nu\ \overline{L^0}$ or $\overline{\nu}L^0$
    - $L^0 \rightarrow e\ W^*$ missing energy and p_t
    - $L^0 \rightarrow \mu\ W^*$ missing energy and p_t
    - $L^0 \rightarrow \tau\ W^*$ missing energy and p_t
    - $L^0 \rightarrow \nu\ Z^*$ missing energy and p_t

In the $e^+e^- \rightarrow L^0\overline{L^0}$ production channel, events can occur where the L^0 and the $\overline{L^0}$ do not decay to the same mixing partner (e μ *or* τ) or through the same mode (charged-current or neutral-current), depending on the model. Such processes have not been considered explicitly in this study. If both the L^0 and the $\overline{L^0}$ decay through a charged-current mode, but to different mixing partner (e.g. $L^0 \rightarrow e\ W^*$, $\overline{L^0} \rightarrow \tau\ W^*$), then the acceptance is at least as large as the lesser of the two single mode acceptances ($L^0 \rightarrow \tau\ W^*$, $\overline{L^0} \rightarrow \tau\ W^*$) or ($L^0 \rightarrow e\ W^*$, $\overline{L^0} \rightarrow e\ W^*$). If the L^0 decays through both charged-current modes (with 2/3 branching ratio) and neutral-current modes (with 1/3 branching ratio) as expected in one model [4], then a conservative upper limit on the production rate is 9/4 times the limit obtained assuming pure charged-current decays.

The partial width for the decay

$$L^0 \rightarrow l^- W^* \rightarrow l^- l'^+ \nu_{l'}$$

is given by:

$$\Gamma(L_0 \rightarrow l^- l'^+ \nu_{l'}) = |U_{lL}|^2 \frac{G_F^2 M_L^5}{192\pi^3}$$

where $|U_{lL}|^2$ is the coupling strength of the neutral heavy lepton L^0 to the light generation ($l,l' = e$, μ, or τ). For heavy neutral lepton production via $e^+e^- \rightarrow L^0\overline{L^0}$, if the value of $|U_{lL}|^2$ is sufficiently small, the heavy leptons could escape detection because of a long lifetime. From a Monte Carlo calculation incorporating our charged track selection criteria, the effect of finite neutral heavy lepton lifetimes on acceptance has been estimated. Figure 2 shows the mixing parameter value at which we expect a less than 10% loss in detection efficiency plotted as a function of the heavy lepton mass. For $|U_{lL}|^2$ values greater than 10^{-7} (M_L=25 GeV/c^2) to 10^{-9} (M_L= 45 GeV/c^2), the acceptance losses are very small.

For heavy lepton production via $e^+e^- \rightarrow \nu\, \overline{L^0}$ or $\overline{\nu}L^0$, the parameter $|U_{lL}|^2$ also enters the cross section. One finds that if $|U_{lL}|^2$ is large enough to permit production at the sensitivity of this experiment, then the lifetime is very short and there is no loss in acceptance. Ignoring phase space factors, the production of one event in our data sample corresponds to a $|U_{lL}|^2$ value of 2×10^{-4}. At M_L=20 GeV/c^2 and $|U_{lL}|^2 = 2 \times 10^{-4}$, the mean decay length is 3.2 μm [7] where the heavy lepton decays through virtual W modes.

In each of the two searches, some common event selection criteria were applied. These included 1) cuts to ensure nominal operation of the relevant detector elements, 2) cuts to suppress backgrounds from cosmic rays and beam–gas interactions, and 3) cuts to ensure accurate event reconstruction. A detailed description of these cuts has been presented elsewhere [8].

Missing Energy/Momentum Search

The missing energy/momentum search is used to look for $e^+e^- \rightarrow \nu\, \overline{L^0}$ or $\overline{\nu}L^0$ events and for $e^+e^- \rightarrow L^0\overline{L^0}$ events where the neutral heavy lepton decays through $L^0 \rightarrow \nu_l Z^*$. The search is based on the total visible energy in the event and on the component of the total momentum transverse to the beam direction. These two quantities are calculated by summing the four–momenta derived from each accepted track in the jet chamber and from each cluster in the lead–glass electromagnetic calorimeter, assuming massless particles. If a cluster has one or more tracks associated to it, only the excess of the cluster energy over the sum of the momenta of the associated tracks is included in the sum (this is to avoid double–counting of energy). The four–momentum sum is used to define the total visible energy (E_{vis}), the magnitude (p_t) of the total momentum transverse to the beam, and the direction of the missing momentum. Comparison of E_{vis} and p_t distributions from the data and hadronic Z^0 Monte Carlo events are in good agreement [8].

To eliminate backgrounds from hadronic Z^0 decays, events are required to have a measured $p_t \geq 0.17 E_{vis} + 6.0$ GeV/c, (E_{vis} in GeV) and a visible energy $E_{vis} \leq 80.0$ GeV. To suppress background from events with undetected energetic particles escaping down the beam pipe, events are rejected if the energy measured in the forward detector exceeds 5.0 GeV.

Background from τ-pair production is eliminated by requiring the thrust of the event (calculated from charged tracks alone) to be less than 0.95.

The remaining background comes primarily from hadronic events in which a mismeasurement of the energy of a jet leads to an artificial missing momentum. This missing momentum tends to lie along the direction of other particles detected in the event. Therefore, we require that there be no energetic detected particles produced in the direction of the missing momentum. We calculate the total energy of charged tracks and electromagnetic clusters within a cone of 30° half-angle around the direction of the missing momentum, and require both of these cone energies E_{cone} to be less than 1 GeV.

Figure 3a shows the distribution of events in visible energy vs p_t after the other cuts have been applied. Two events are selected by the missing energy/momentum search. Both are multihadron events with large visible energy (69 and 67 GeV), missing momentum (20 and 18 GeV/c), and charged–track multiplicity (33 and 28). The observed events are consistent with background expected from hadronic Z^0 decay. Based on Monte Carlo studies we expect to observe 1.3±0.8 such events. Figure 3b shows an example of the visible energy vs p_t distribution for a neutral heavy lepton signal. The acceptance and sensitivity to neutral heavy lepton events are discussed below. Upper limits from the missing energy and momentum search are based on 6.3 expected events (95% CL upper limit on 2 observed events).

Isolated Track Search

The second event selection method is used to search for events of the type $e^+e^-\to L^0\overline{L^0}$ where the neutral heavy lepton decays through $L^0\to l\ W^*$, $l\ =\ e\ \mu$ *or* τ. It requires that a candidate event have a minimum of four charged tracks, each with momentum greater than 1 GeV/c, two of which are isolated tracks. One of the isolated tracks must be identified as a lepton. Only tracks with reconstructed momentum greater than 5 GeV/c and $|\cos\theta| < 0.7$, where θ is the polar angle measured with respect to the beam, are considered as isolated track candidates. The track must be associated with a cluster of at least 100 MeV energy in the electromagnetic calorimeter. A minimum-ionizing particle typically deposits 700 MeV in the electromagnetic calorimeter. The isolation requirement is imposed by requiring that within a cone of 30° half–angle around the isolated track (1) the total energy from other charged tracks be less than 1 GeV, and (2) the total energy of electromagnetic clusters, excluding the cluster associated with the track, be less than 2 GeV.

Electron and muon selection criteria have been presented in detail in a previously published search for charged heavy leptons [8]. Briefly summarized, electron identification is based on a match between the track momentum measured in the central tracking system and the energy measured in the electromagnetic calorimeter. In addition, an electron is required to have a transverse shower size (number of lead glass blocks hit) and longitudinal shower size (penetration into the hadron calorimeter) consistent with an electromagnetic shower. Muon tracks are identified by a small energy deposition in the electromagnetic calorimeter and by penetration into the hadron calorimeter and muon chamber systems. Based on an analysis of independently selected samples of $e^+e^-\to e^+e^-$, $e^+e^-\to\mu^+\mu^-$, and $e^+e^-\to\tau^+\tau^-$ events, electron and muon identification efficiencies are 86±3% and 92±3% respectively.

After the above cuts are applied to the data, five events remain. Four of these events are consistent with background from $e^+e^-\ \to\ l^+l^-\gamma$, with the photon converting to an e^+e^- pair. The fifth event appears to be $\mu^+\mu-\pi^+\pi^-$, where the pion pair has an invariant mass consistent with a ρ. All of these events are removed by requiring that the transverse mass of all charged tracks with $p > 1$ GeV/c, excluding the two isolated tracks, be greater than 1.5 GeV/c^2. This additional cut reduces the efficiency for detecting $L^0\bar{L}^0$ events by less than 10%..

Limits derived from this search are based on 3.00 events (95% CL upper limit for zero observed events). Based on Monte Carlo studies, we expect to observe 0.6±0.6 background events from hadronic Z^0 decays.

4 Monte Carlo Generation

The $e^+e^-\rightarrow L^0\overline{L^0}$ heavy lepton samples were produced using a modified version of the TIPTOP [10] Monte Carlo program. TIPTOP includes mass effects, initial-state radiative corrections and spin-spin correlations among heavy lepton decay products. The program was modified to include the decay $L^0\rightarrow\nu_l Z^*$, by generalizing the L^0 decay matrix element. Additional modifications were necessary to simulate $e^+e^-\rightarrow\nu\ \overline{L^0}$.

Events were processed through the fast version of the OPAL detector Monte Carlo code. This code selects detector signals from parameterized distributions derived from the full shower OPAL package. Comparison with selected samples produced using the full showering code gave consistent results. In calcutating upper limits on neutral heavy lepton production, we have included a 5% uncertainty in the acceptance calculations, to which we have added a 3% uncertainty in the luminosity, to get a total uncertainty of 8% on the expected number of signal events.

5 Results

The acceptances have been calculated as a function of neutral-heavy-lepton mass (M_L) for each of the two production modes $e^+e^-\rightarrow L^0\overline{L^0}$ and $e^+e^-\rightarrow\nu\ \overline{L^0}$ (or $\bar{\nu}L^0$). The results are shown for each of the four heavy-lepton decay modes ($L^0\rightarrow e\ W^*$, $\mu\ W^*$, $\tau\ W^*$, and $\nu\ Z^*$) in Figures 4a and 4b.

In the $L^0\overline{L^0}$ final state the acceptance is smaller for the $L^0\rightarrow\tau\ W^*$ mode then for the $L^0\rightarrow e\ W^*$ or $L^0\rightarrow\mu\ W^*$ modes. The large branching fraction of the τ to hadronic modes results in many of the τ decay combinations not satisfying the isolated track selection requirements.

The number of events expected in the data sample is given by:

- $N_{L\bar{L}} = A_{L\bar{L}}L\sigma_{L\bar{L}}$
  - $A_{L\bar{L}}$ - acceptance
  - L - luminosity
  - $\sigma_{L\bar{L}}$ - cross section

then:

$$\frac{\sigma_{L\bar{L}}}{\sigma_{Had}} = \frac{\Gamma(Z_0\rightarrow L^0\,\overline{L^0})}{\Gamma(Z^0\rightarrow hadrons)} = \frac{N_{L\bar{L}}A_H}{N_{Had}A_{L\bar{L}}}$$

Using this formula, the acceptance curves were converted to 95% confidence level upper limits on $\Gamma(Z_0\rightarrow L^0\ \overline{L^0})\,/\,\Gamma(Z^0\rightarrow hadrons)$ vs M_L. The results are shown in Figures 5a. The limits can be compared with the expected branching ratio for standard model coupling in $L^0\overline{L^0}$ production shown in Figure 1. In the standard model, the number of fourth-generation massive neutrinos produced can be calculated as a function of mass, summing the production cross section times the integrated luminosity at each beam energy. From this calculation and the detection efficiencies shown in Figure 4a, we can set 95% CL limits on the mass of a standard model L^0:

$$M_{L^0} > 46.3\ \mathrm{GeV}/c^2,\ \text{if } L^0 \text{ mixes with } e \text{ or } \mu,$$

$$M_{L^0} > 45.7\ \mathrm{GeV}/c^2,\ \text{if } L^0 \text{ mixes with } \tau.$$

These limits are valid only if the mixing at a given L^0 mass is greater than the value shown in Figure 2.

The limits on the branching ratios for the $e^+e^-\rightarrow\nu\ \overline{L^0}$ (or $\bar{\nu}L^0$) process for the four L^0 decay modes are shown in Figure 5b. The neutrino energy decreases as the neutral heavy lepton mass (M_L) increases. This results in a decreased acceptance at high M_L in the $L^0\rightarrow e$, μ, or τ W^* modes, since it is less likely that the missing energy and p_t criteria are satisfied. Neutral heavy leptons are excluded in Z^0 decay at the level of 10^{-3} to 10^{-4} of $Z^0\rightarrow$hadrons, depending on the neutral heavy lepton mass and decay mode.

In the see–saw model, the production rate depends on both the mass M_{L^0} and the mixing $|U_{lL}|^2$. From the branching ratio limits given in Figure 5b, we can set limits on $|U_{lL}|^2$ as a function of M_{L^0}. If we assume that the L^0 decays through the charged–current with 2/3 branching ratio and through the neutral current with 1/3 branching ratio, we obtain the 95% CL limits shown in Figure 6 for e, μ, and τ mixing. The regions above the curves are excluded. The unitarity limits [4] for each type of mixing are shown for comparison. The search for $e^+e^-\rightarrow\nu\ L^0$ (or $\bar{\nu}L^0$) events will be of continuing interest as the accumulation of data at LEP allows greater sensitivity.

6 Acknowledgments

It is a pleasure to thank the LEP Division for the smooth running of the accelerator and for continuing close cooperation with our experimental group. In addition to the support staff at our own institutions we are pleased to acknowledge the following: The Bundesministerium für Forschung und Technologie, FRG, The Department of Energy, USA, The Institut de Recherche Fondamentale du Commissariat a l'Energie Atomique, The Israeli Ministry of Science, The Minerva Gesellschaft, The National Science Foundation, USA, The Natural Sciences and Engineering Research Council, Canada, The Japanese Ministry of Education, Science and Culture (the Monbusho) and a grant under the Monbusho International Science Research Program, The Science and Engineering Research Council, UK and The A. P. Sloan Foundation.

References

[1] More recent experimental results can be found in:
W. Bartel *et al.* Phys. Lett. **123B** (1983) 353.
D. Errede *et al.* Phys. Lett. **149B** (1984) 519.
C. Wendt *et al.* Phys. Rev. Lett. **58** (1987) 1810.
H. J. Behrend *et al.* Z. Phys. **C41** (1988) 7.
K. Abe *et al.* Phys. Rev. Lett. **61** (1988) 915.
C. Akerlof *et al.* Phys. Rev. **D37** (1988) 577.
N. M. Shaw *et al.* Phys. Rev. Lett. **63** (1989) 1342.
G. S. Abrams *et al.* Phys. Rev. Lett. **63** (1989) 2447.
C. K. Jung *et al.* Phys. Rev. Lett. **64** (1990) 1091.
D. Decamp *et al.* CERN-EP/89-165. (Submitted to Phys. Lett. B)

[2] OPAL Technical proposal (1983) and CERN/LEPC/83-4.

[3] F. J. Gilman, Comm. Nucl. Part. Phys. **16** (1986 231.

[4] M. Gronau,C. N. Leung and J. L. Rosner, Phys. Rev. **D29** (1984) 2539.

[5] M. Dittmar, A. Santamaria, M. C. Gonzalez-Garcia and J. F. F. Valle CERN-EP/89-50.

[6] M.Z. Akrawy *et al.* CERN-EP/09-27. (Submitted to Phys. Lett. B)

[7] V. Barger,W.Y. Keung, and R.J.N. Phillips, Phys. Lett. **141B** (1984) 126.

[8] M.Z. Akrawy *et al.* CERN-EP/90-09. To appear in Phys. Lett. **240B** (1990).

[9] M.Z. Akrawy *et al.* CERN-EP/89-147. (Submitted to Phys. Lett. B)

[10] S. Jadach and J. Kuhn, MPI-PAE/PTh 64/86.

[11] M. Bengtsson and T. Sjostrand, Nucl. Phys. **B289** (1987) 810.
T. Sjostrand, Comp. Phys. Comm. 39 (1986) 345; JETSET, Version 7.1.

[12] R. Brun, F. Bruyant, M. Maire, A. C. McPherson and P. Zanarini, *GEANT3*, CERN DD/EE/84-1 (1987).

Figure Captions

FIGURE 1: The partial width $\Gamma(Z^0 \rightarrow L^0 \overline{L^0})$ vs M_L or equivalently $\frac{\Gamma(Z_0 \rightarrow L^0\, \overline{L^0})}{\Gamma(L^0 \rightarrow hadrons)}$ *vs* M_L for standard model coupling

FIGURE 2: For a given M_L, at a value of $|U_{lL}|^2$ larger than the value plotted, the finite heavy lepton lifetime would result in a detection efficiency loss less than 10%. The mass limits of Figures 5a and 5b assume no loss due to finite lifetimes.

FIGURE 3: a) visible energy vs p_t for the data after the thrust, cone energy, and forward detector energy cuts have been applied b) the equivalent plot for a 60 GeV/c^2 mass neutral heavy lepton $Z^0 \rightarrow \nu\ \overline{L^0}$ or $\bar{\nu} L^0$ where $L^0 \rightarrow e\ W^*$

FIGURE 4: (a) Acceptance vs M_z for the process $e^+e^- \rightarrow L^0\overline{L^0}$, where the neutral heavy lepton decays via (1) $L^0 \rightarrow e\ W^*$, (2) $L^0 \rightarrow \mu\ W^*$, (3) $L^0 \rightarrow \tau\ W^*$, or (4) $L^0 \rightarrow \nu\ Z^*$. (1),(2), and (3) are based on the isolated track search. (4) is based on the missing energy and p_t search. (b) Acceptance vs M_z for the process $e^+e^- \rightarrow \nu\ \overline{L^0}$ or $\bar{\nu} L^0$, where the neutral heavy lepton decays via (1) $L^0 \rightarrow e\ W^*$, (2) $L^0 \rightarrow \mu\ W^*$,(3) $L^0 \rightarrow \tau\ W^*$, or (4) $L^0 \rightarrow \nu\ Z^*$. All are based on the missing energy and p_t search.

FIGURE 5: (a) 95% CL upper limit on $\frac{\Gamma(Z_0 \rightarrow L^0\, \overline{L^0})}{\Gamma(L^0 \rightarrow hadrons)}$ *vs* M_l for (1) $L^0 \rightarrow e\ W^*$, (2) $L^0 \rightarrow \mu\ W^*$, (3) $L^0 \rightarrow \tau\ W^*$, or (4) $L^0 \rightarrow \nu\ Z^*$. (1),(2), and (3) are based on the isolated lepton search. (4) is based on the missing energy and p_t search. (b) 95% CL upper limit on $\frac{\Gamma(Z_0 \rightarrow \nu\, \overline{L^0}\ or\ \bar{\nu} L^0)}{\Gamma(L^0 \rightarrow hadrons)}$ *vs* M_L for (1) $L^0 \rightarrow e\ W^*$, (2) $L^0 \rightarrow \mu\ W^*$,(3) $L^0 \rightarrow \tau\ W^*$, or (4) $L^0 \rightarrow \nu\ Z^*$. All are based on the missing energy and p_t search.

FIGURE 6: The 95% CL limits on $|U_{lL}|^2$ as a function of M_{L^0} for e, μ, and τ mixing. We assume that the L^0 decays through the charged–current with 2/3 branching ratio and through the neutral current with 1/3 branching ratio. The regions above the curves are excluded. The unitarity limits [4] for each type of mixing are shown for comparison.

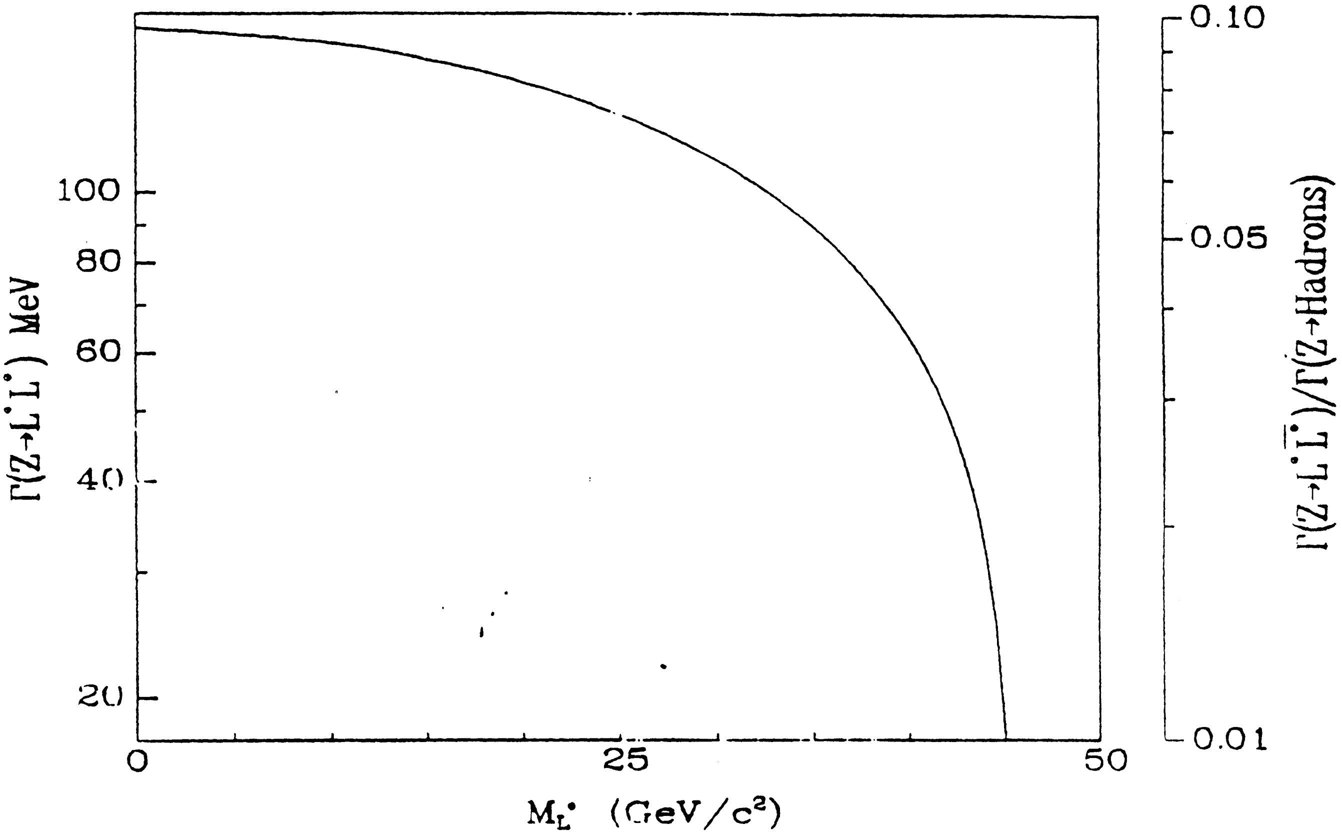

100
80
60
40
20
Γ(Z→L*L̄*) MeV
0.10
0.05
0.01
Γ(Z→L*L̄*)/Γ(Z→Hadrons)
0
25
50
M_L* (GeV/c²)

FIGURE 1

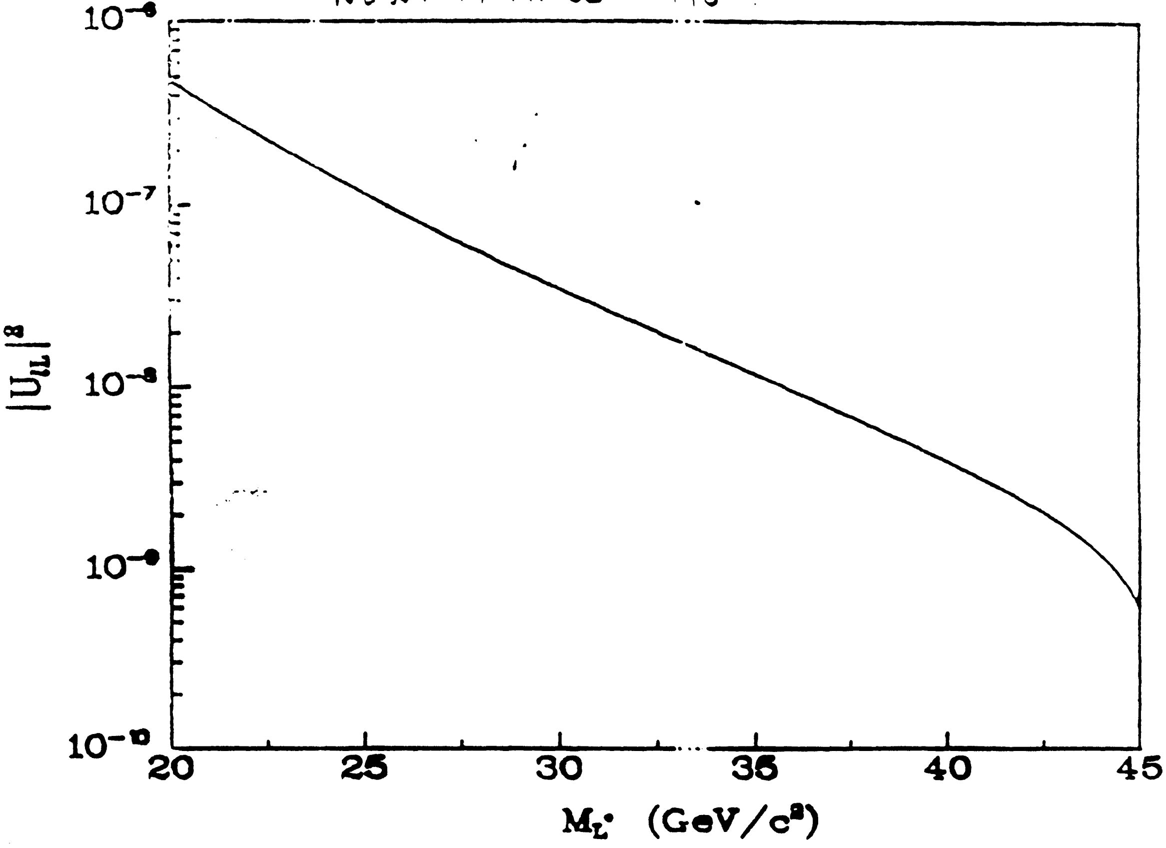

NEW: 14 MARCH 1990

FIGURE 2

NEW: MARCH 15, 1990

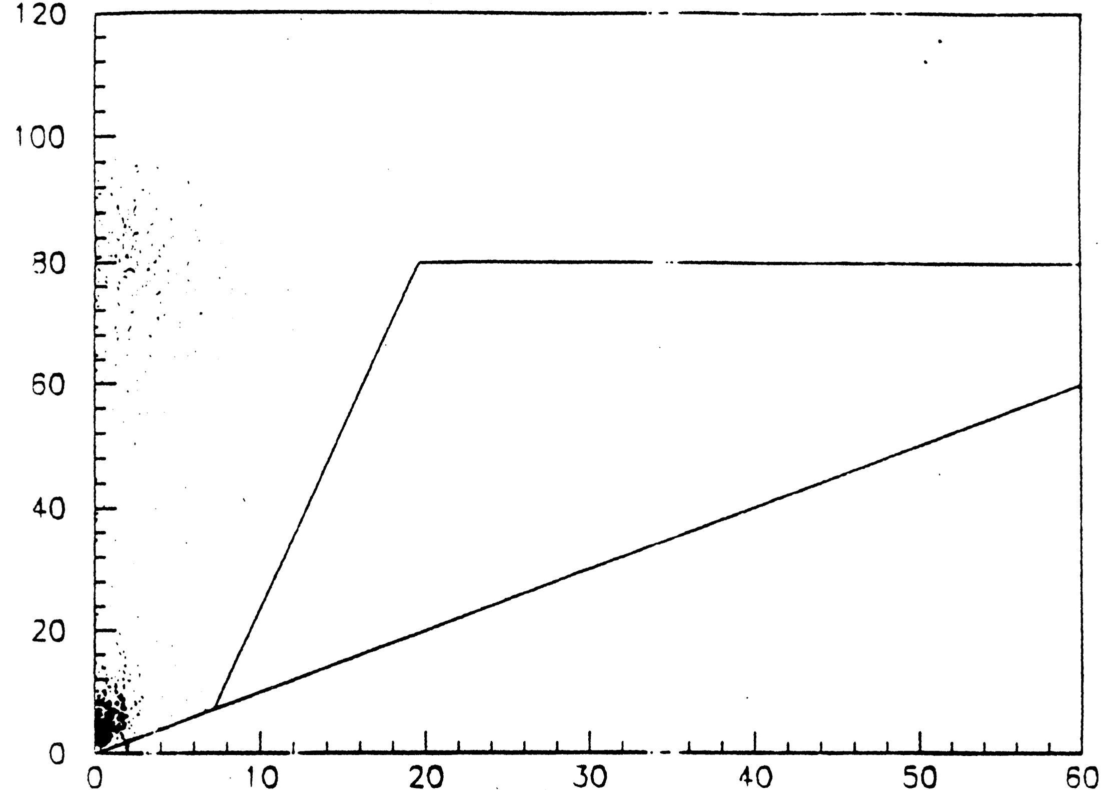

E_{vis} vs. P_T (data) after thrust and isolation cuts

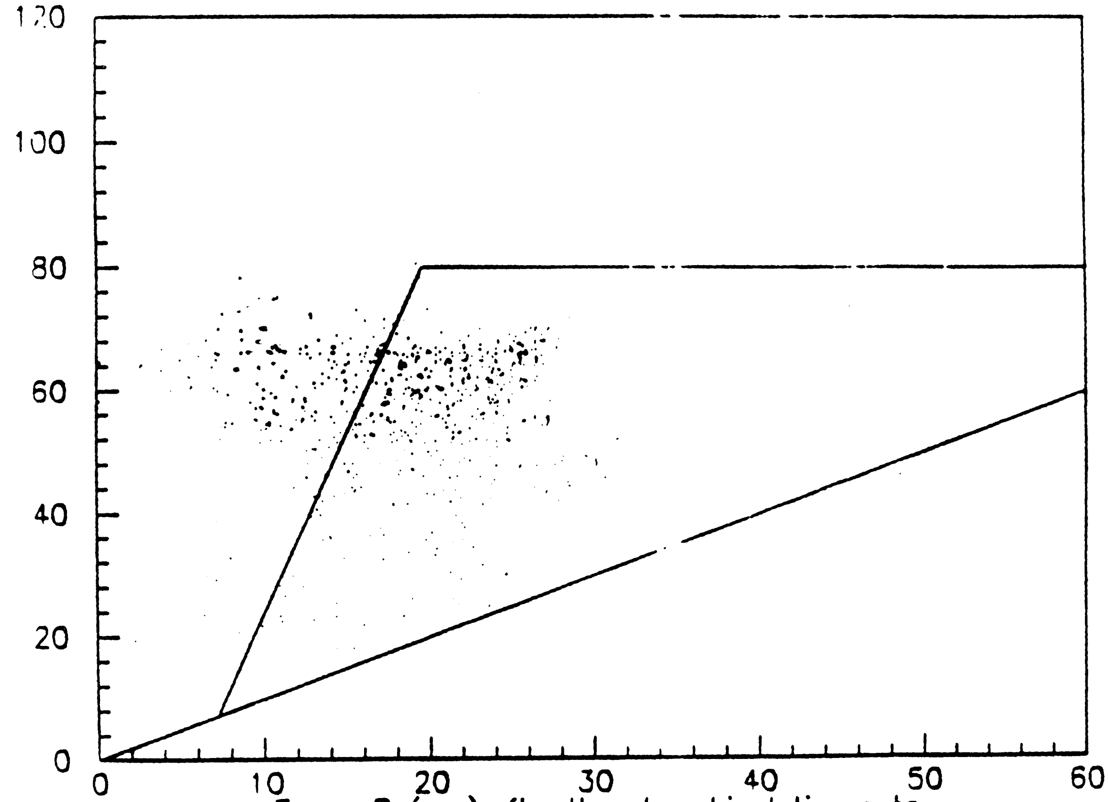

E_{vis} vs. P_T (mc) after thrust and isolation cuts

Figure 3.

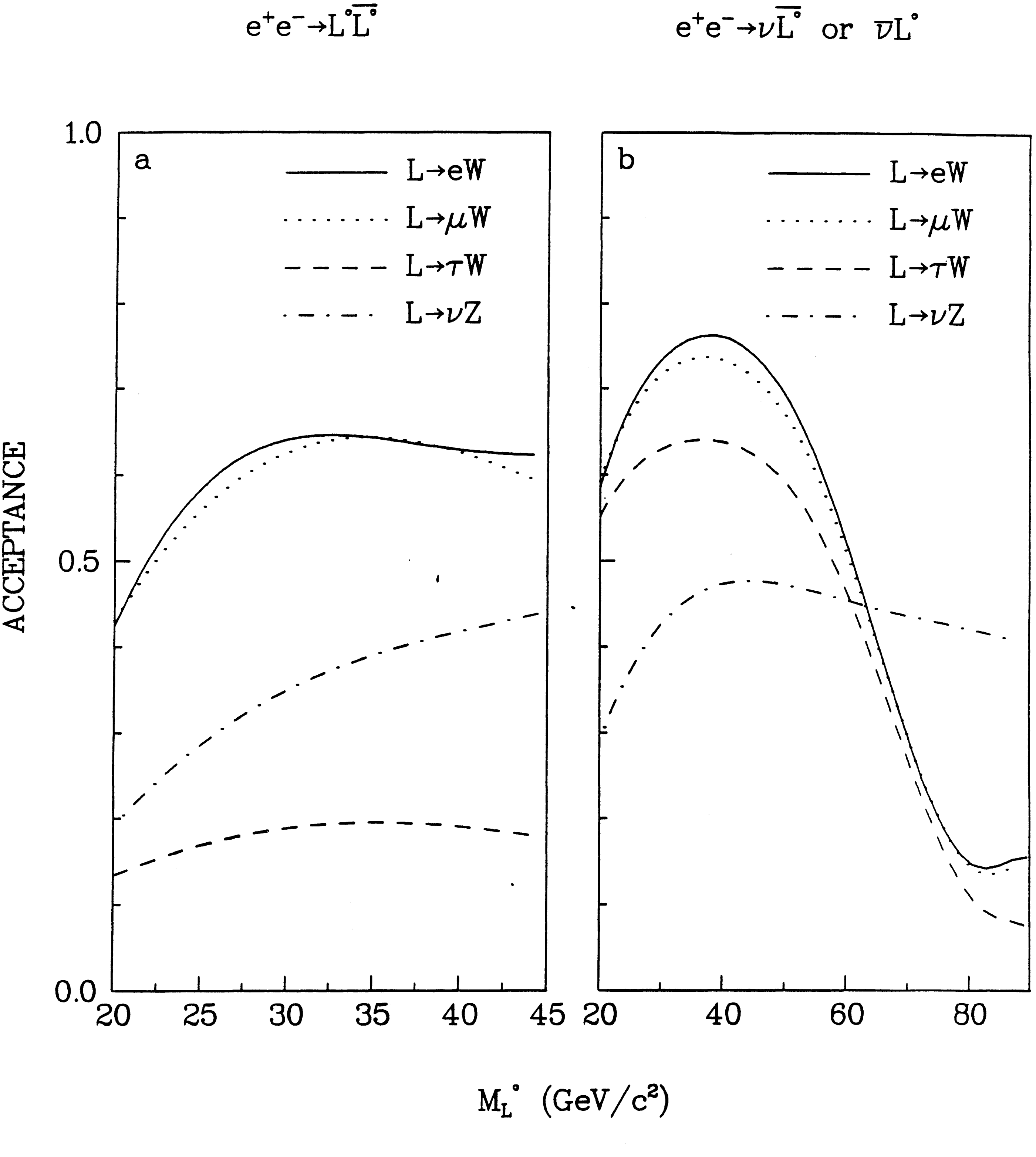$e^+e^- \to L^\circ\overline{L^\circ}$
$e^+e^- \to \nu\overline{L^\circ}$ or $\overline{\nu}L^\circ$
a
b
L→eW
L→μW
L→τW
L→νZ
ACCEPTANCE
1.0
0.5
0.0
20
25
30
35
40
45
20
40
60
80
M_{L° (GeV/c^2)

FIGURE 4

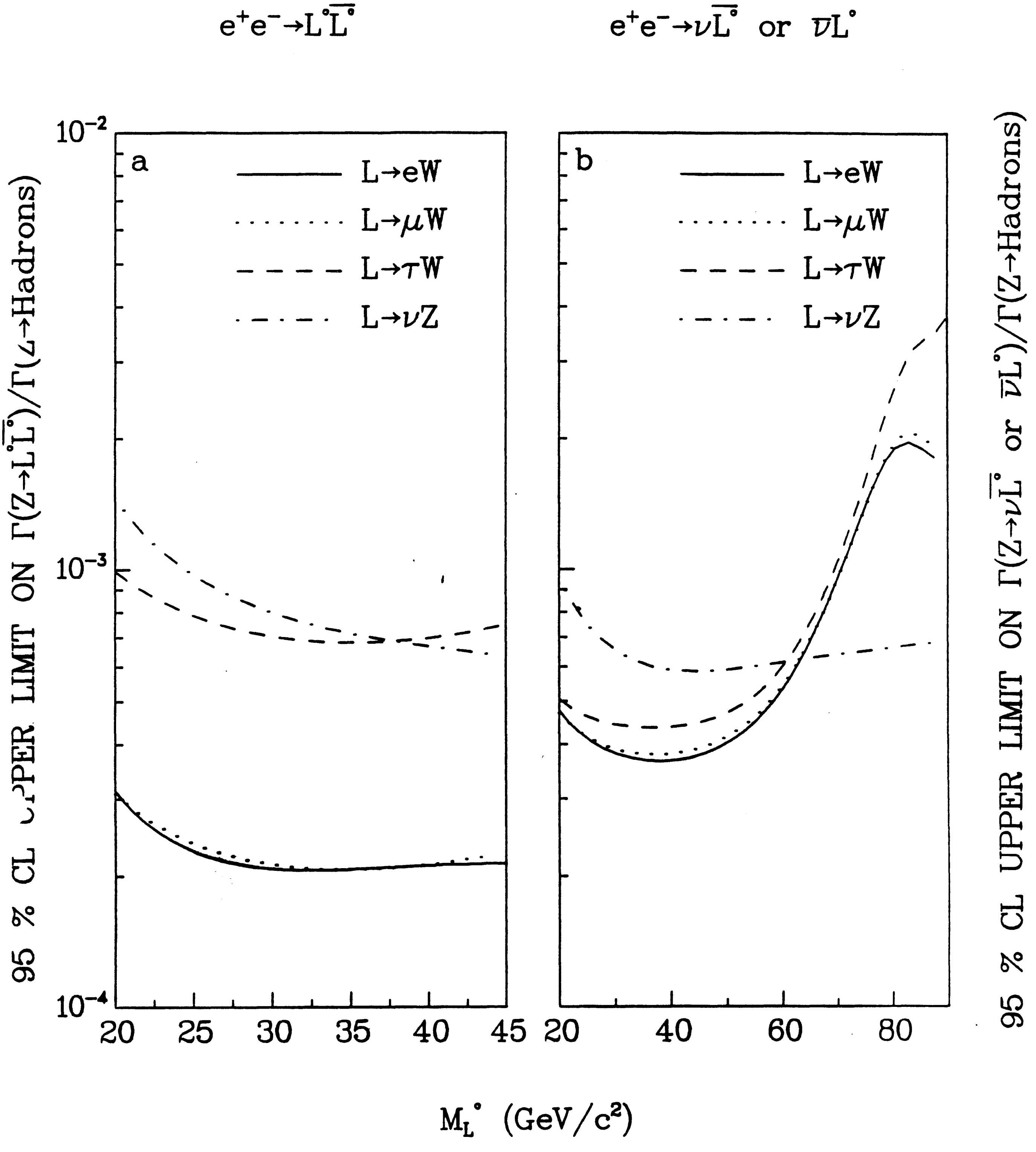

e^+e^-→L°L°‾
e^+e^-→νL°‾ or ν̄L°
10^-2
10^-3
10^-4
a
b
L→eW
L→μW
L→τW
L→νZ
95 % CL UPPER LIMIT ON Γ(Z→L°L°‾)/Γ(Z→Hadrons)
95 % CL UPPER LIMIT ON Γ(Z→νL°‾ or ν̄L°)/Γ(Z→Hadrons)
20
25
30
35
40
45
20
40
60
80
M_L° (GeV/c²)

FIGURE 5

Fig. 6 — 95 percent CL limit, $Z-\nu L^0$